Circular poly (ethylene terephthalate) with lignin-based toughening additives

Chemical Engineering Journal 504 (2025) 158255

Contents lists available at ScienceDirect

Chemical Engineering Journal

journal homepage: www.elsevier.com/locate/cej

Circular poly(ethylene terephthalate) with lignin-based toughening additives

Xue Wan [a,b,g], Li-Yang Liu [b,c,d,e,*], Muzaffer A. Karaaslan [b], Qi Hua [b], Fei Shen [a], Mika Sipponen [e,f,**], Scott Renneckar [b,***]

[a] Sichuan Provincial Engineering Research Centre of Pollution Control in Agriculture, College of Environmental Sciences, Sichuan Agricultural University, Chengdu 611130, PR China
[b] Advanced Renewable Materials Lab, Department of Wood Science, University of British Columbia, Vancouver V6T 1Z4, Canada
[c] Department of Chemistry and Chemical Engineering, Chalmers University of Technology, Gothenburg SE-41296, Sweden
[d] Wallenberg Wood Science Center, Department of Chemistry and Chemical Engineering, Chalmers University of Technology, Gothenburg SE-41296, Sweden
[e] Department of Materials and Environmental Chemistry, Stockholm University, Stockholm 11418, Sweden
[f] Wallenberg Wood Science Center, Department of Materials and Environmental Chemistry, Stockholm University, Stockholm 11418, Sweden
[g] Institute of Agricultural Resources and Environment, Sichuan Academy of Agriculture Sciences, Chengdu 610066, PR China

ARTICLE INFO

Keywords:
Poly (ethylene terephthalate)
Lignin
Modification
Circularity
Toughening additives

ABSTRACT

Creating sustainable plastics demands an efficient strategy to reduce the carbon footprint and enhance the circularity of widely used materials. Inspired by the structure of plant cell walls, renewable lignin macromolecules are modified with benzoate ethyl functional groups and combined with semi-crystalline poly(ethylene terephthalate) (PET) at a 10 % weight ratio. This process significantly improves the toughness (+97 %) and strength (+ 56 %) of PET while also reducing greenhouse gas emissions (−17 %) and promoting circularity, outperforming traditional toughening agents. Our in-depth analysis indicates that benzoate ethyl lignin derivatives exhibit improved thermal stability and controllable physical structure. The newly added benzoate ethyl groups are similar to the fundamental units in PET, facilitating the formation of micro-scale particles within the PET matrix and improving their crystallinity and mechanical performance. The resulting composite can be reprocessed at least three times, representing a significant breakthrough in mechanical processing of thermoplastics. Therefore, this study presents a promising approach to utilizing lignin biopolymer and waste PET for advanced materials with positive environmental footprints.

1. Introduction

Plastics from petroleum-based precursors have versatile applications, but their improper end-of-life disposal causes widespread environmental contamination of land and sea [1]. Poly(ethylene terephthalate) (PET), with an annual production of 24 million tons, is the fourth largest type of synthetic plastics [2], and will have continually growing demands because of its broad applications, e.g., single-use food packaging and textile manufacturing. Their hydrolyzable ester linkages and thermal resistance make it possible to recycle PET in either mechanical or solvent-based chemical methods, or a combination thereof, and in the future, potentially aided with recently discovered hydrolytic enzymes [3]. As such, it has attracted growing interest in creating circular materials from these ubiquitous plastics [4]. Most existing methods aim to reuse or regenerate this plastic for the same industrial fields [5]. Nonetheless, the challenges concerning a costly sorting process, the reduction of molar mass during mechanical recycling, and the utilization of organic solvents in harsh conditions for depolymerization come together to restrain the recycling process. New PET bottles on the market only contain around 17 % recycled plastics, although the beverage deposit refund schemes have been deployed in Europe, leading to a 50 % - 90 % recycling rate depending on the countries [6].

An alternative strategy is to convert the recycled polymers to materials of higher value – the upcycling process [7]. Incorporating

* Corresponding author at: Department of Chemistry and Chemical Engineering, Chalmers University of Technology, Gothenburg SE-41296, Sweden.
** Corresponding author at: Department of Materials and Environmental Chemistry, Stockholm University, Stockholm 11418, Sweden.
*** Corresponding author at: Advanced Renewable Materials Lab, Department of Wood Science, University of British Columbia, Vancouver V6T 1Z4, Canada.
E-mail addresses: liyang.liu@chalmers.se (L.-Y. Liu), mika.sipponen@mmk.su.se (M. Sipponen), scott.renneckar@ubc.ca (S. Renneckar).

https://doi.org/10.1016/j.cej.2024.158255

Available online 4 December 2024

renewable toughening additives can be a straightforward upcycling strategy [8]. These additives can compensate for the decreasing mechanical performance after the mechanical recycling process or endow the plastics with advanced performance for new applications, such as the honeycomb cores of automobiles and wind turbine foams [9]. A substantial mechanical performance enhancement can reduce the mass of material required to meet a loading function. With a high loading level but a low cost, toughening additives can decrease the overall cost of PET-based materials. Some additives with antioxidant performance can inhibit the degradation of plastics, enhancing their resistance during mechanical reprocessing. All of these can help achieve the ambitious goal of the EU package and package waste regulation (PPWR) for 70 % of packaging and 55 % of plastics to be recyclable by 2030 [10]. However, much research has focused on petroleum-based synthetic rubbers and inorganic additives [11,12]. Synthetic rubber is usually costly to prepare due to toxic non-renewable precursors. Processing inorganic nanofillers in materials requires special conditions for particle exfoliation and dispersion. As such, upcycling PET requires researchers to explore toughening additives from renewable resources and develop more effective processing methods to improve their interfacial adhesion with the PET.

Lignin is a branched macromolecule, accounting for 15 % − 30 % of terrestrial plants (i.e., wood and agricultural residue) by weight. As a matrix material surrounding semicrystalline cellulose, lignin is crucial in forming an exquisite architecture in the cell wall and enhancing its mechanical performance [13]. Kraft lignin from the pulping process has attracted growing interest in developing bioproducts due to their renewability, abundance, and cost-effectiveness [14,15]. Blending renewable kraft lignin with semi-crystalline PET can be a promising strategy for meeting the above needs in upcycling existing PET [16,17]. Several critical factors should be considered when lignin is directly used as an additive for PET. Unmodified softwood kraft lignin is received as irregular microparticles with complex composition, broad molecular weight distribution, and numerous surface functional groups (phenol, carboxylic acid, and aliphatic hydroxyl groups) [18] This complexity will lead to significant compatibility issues with the PET matrix. Also, several reactions can occur under high processing temperatures (PET melting temperature is 260 °C), such as the cleavage of surface hydroxyl groups, the degradation of Xylan, and the radical condensation attributed to the reactive phenol groups [19] More importantly, technical lignin is isolated with a broad molecular weight distribution; high molecular weight means higher glass transition temperature [20], another critical factor influencing their compatibility with the PET matrix. T_g of softwood kraft lignin is 160 °C, much higher than PET (T_g = 82.5 °C) [20] The lower molecular weight with lower T_g can plasticize thermoplastics [21] Finally, the molecular weight of lignin varies depending on the source and isolation method of lignin, causing problems with quality control when blending lignin directly with plastic materials [22].

Herein, we present an efficient and cost-effective upcycling approach to make PET plastics stronger and more eco-friendly by adding modified kraft lignin [23,24]. Firstly, a green and efficient route is developed to convert the underutilized kraft lignin into uniform benzoate ethyl lignin (BELignin) building blocks [25]. The end group of benzoate ethyl groups is akin to the repeating unit of PET that may foster the interfacial adhesion with PET. More efficient use of ethylene carbonate and benzoic acid in a one-pot process can satisfy several fundamental principles of green chemistry (i.e., principles no. 1, 3, 5, 7, and 11). We then blend these BELignins with PET to fabricate a series of LignoPET filaments, followed by a thorough characterization of their morphology, thermal properties, and mechanical performance. The structure–property relationship of LignoPET is investigated to elucidate the reinforcement mechanism. We also perform a cradle-to-gate life cycle carbon footprint assessment on making LignoPET composite, compared with conventional toughening additives such as synthetic rubber and inorganic nanofillers. Compared with native lignin in the cell wall, technical lignin contains phenolic groups, allowing it to be used as an antioxidant that can contribute to the durability and circularity of the resulting composite [26]. The initial reprocessing of LignoPET indicates that BELignin can still enhance its circularity by reprocessing three times, even though the functionalization of phenol groups may lower the antioxidant ability. Results from this study show that BELignin, as a functional additive, can effectively toughen PET, paving the way for the circular economy.

2. Materials and methods

2.1. Raw materials and chemicals

Lignin was received from the West Fraser Corp. (Hinton Pulp, AB, Canada), which adopted the LignoForce™ process to recover lignin powders from a softwood kraft pulping process. The lignin was dried before the modification and characterization. The ethylene carbonate (98 %, Fischer Scientific) was stored in a vacuum oven over the P_2O_5 drying agents to control the moisture content. PET pellets, containing 40 % of recycled PET, were received from the Evian Company. These pellets were dried thoroughly to eliminate the moisture content.

2.2. Synthesis and fractionation of benzoate ethyl lignin (BELignin) derivatives

Step 1 hydroxyethyl modification: 10 g oven-dried lignin powders were mixed with 32 g ethylene carbonate and 1 g Na_2CO_3 in a 100 ml round-bottom Schlenk flask, which owned a sidearm for the emission of CO_2 gas products. The flask was loaded in an oil bath at 120 °C with continuous magnetic stirring. During the modification, the CO_2 gas emission rate was measured by the flow mass meter (Model: FMA 1607 A, Flow range: 0.05—10 SLM, Omega Engineering, Inc.) The HyperTerminal software (Hilgrave Inc.) was employed to record the CO_2 gas emission rate every 30 s, which was plotted in Excel to realize the real-time monitoring process. Real-time monitoring equipment was assembled as shown in Supplementary Figure 1.

Step 2 direct esterification: The flask was immediately lifted from the oil bath while the gas flow rate closed to 0.2 – 0.3 mL min^{-1}. 100 g benzoic acid (ACS reagent, Sigma Aldrich) was added to quench the hydroxyethyl modification and perform the esterification reactions at 170 °C for 48 h in the same oil bath with continual stirring. Once the reaction was finished, the whole flask was immersed in cold water to cool off and measured by the balance to obtain the weight of the reaction mixture (around 120 g).

Step 3 Downward precipitation fractionation: Several trials were performed in advance to find the optimum volume of adding ethanol and mixing temperature. Note that the lignin mixtures will be solidified at room temperature, requiring a specific amount of ethanol to solubilize the mixture. The first ratio between the volume of antisolvent ethanol and the weight of the reaction mixture (v/m) was controlled as 1.25. Specifically, 120 g acquired lignin mixtures were mixed with 150 ml ethanol, followed by continuous stirring at 35 °C. The fractionated BELignin (F1) was obtained by centrifugation (4000 rpm, 10 min, and 35 °C). The supernatant was mixed with another 30 ml ethanol (v/m = 1.5) and stirred for 30 min at 35 °C. After the centrifugation, fractionated BELignin (F2) was received. The supernatant was mixed with another 60 ml ethanol (v/m = 2) and followed with centrifugation to precipitate fractionated BELignin (F3) and related supernatant. Repeating this process by adding 120 ml ethanol (v/m = 3) and another 120 ml ethanol (v/m = 4) could acquire fractionated BELignin (F4) and fractionated BELignin (F5), respectively. All fractionated lignin (F1 − F5) was washed with 3 × 50 ml warm ethanol and dried in a desiccator over P_2O_5. All the centrifugation processes were carried out within conditions (4000 rpm, 10 min, and 35 min). The whole process was repeated in triplicate. The supernatant from the last fractionation and the washing ethanol were all collected for ethanol recovery and reuse. The solid residue (mainly containing benzoic acid) was dried for subsequent analysis.

2.3. Characterization of lignin resources

The actual yield for fractionated lignin was calculated considering the effects of additional functional groups. A detailed calculation equation is explained in our previous studies [25]. Functional hydroxyl groups on the lignin surface are characterized by the ^{31}P nuclear magnetic resonance (NMR). Molecular weight and conformation for different fractions of lignin were thoroughly characterized by gel permeation chromatography (GPC) combined with multiple detectors, including multiangle light scattering (MALS), viscometer (VI), and differential refractive index (dRI) [27]. Thermal stability for the lignin in terms of temperature at 5 % weight loss and temperature at maximum weight loss was characterized by thermal gravimetric analysis (TGA). Glass transition temperature for different lignin fractions were characterized by differential scanning calorimetry (DSC). Our previous studies have described the methodologies (sample preparation, instrument parameters, and data analysis methods) in detail [25,28].

2.4. Thermal blending lignin with poly (ethylene terephthalate) using extruder

A series of PET filaments were fabricated through a conical twin screw micro compounder (Xplore MC 15HT, Netherlands) combined with a microfiber line. The chamber temperature was set to 245 °C, 250 °C, and 265 °C starting from top to bottom, and the chamber outlet temperature was set to 258 °C. During blending, the nitrogen gas was continuously purged into the chamber to avoid the thermo-oxidative degradation of lignin and PET. Different lignin resources, including BELignin (F1-F5) and unmodified lignin, were blended with PET pellets at weight percentage (10 %). The screw speed was set at 100 rpm for 10 min, ensuring a thorough mix. After blending, the screw speed was decreased to 5 rpm, and the filaments were extruded by wounding onto a roller (7.5 cm) with a winding speed of 8 m min^{-1} and maintaining a consistent draw ratio [29]. The same compounding conditions were applied to reprocess these filaments 3 times.

2.5. Characterization of LignoPET filaments

Dynamic mechanical analysis equipped with a tension clamp (TA Q800 Instruments, Waters Corp.) was first used to analyze yield strength and Young's modulus. The fibers were cut in pieces approximately 2 cm long and their diameters were measured using an optical microscopy. The cross-section was assumed to be circular. Each filament was loaded onto the tension clamp with a preload force 0.01 N. The stress–strain curves were collected by stretching the filament with the ramp force 3.0 N min^{-1} until reaching the maximum force (18 N).

Complete stress–strain curves were measured by the Instron tensile testing machine, according to the ASTM C1557 [30]. 2 cm of filaments were pasted onto small pads of abrasive paper (ca. 3 mm × 4 mm), leaving a 10 mm long section of fiber available. Samples were loaded into an Instron tensile clamp and tested at a speed of 25 mm/min until it has broken. The stress–strain curves were then recorded to measure the yield strength, Young's modulus, and Elongation at break (E.B.%).

These filaments' surface morphology and cross-section were observed using an optical microscope (equipment with an Olympus camera) and scanning electron microscope (Hitachi SU3500, 2 kV accelerating voltage). For the former, the filament was embedded in epoxy resin and cut into ~ 100 μm thick slices using a microtome for the cross-section observation. Callen's image processing software was harnessed to measure the size of filaments and lignin particles. For the latter one, filaments were frozen, then bent or cut in liquid nitrogen to observe their cross-section. Before the SEM imaging, filaments were mounted onto metal holders with carbon tape and sputter-coated with iridium.

The melting and crystallization behaviours of PET filaments were studied by the differential scanning calorimetry (DSC, TA 1000) at a cooling and heating rate of 10 K/min. Samples were first heated to 300 °C to analyze the cold crystallization (T_{cc}), and melting peaks (T_m). The enthalpy of melting (ΔH_m) and cold crystallization (ΔH_c) are determined by integrating the areas (J/g) under the peak. The filaments were further cooled down to 50 °C to record the crystallization peaks (T_c). The degree of crystallinity (X_c) was calculated as ($\Delta H_m - \Delta H_c$) / [(1-W_{lignin}) × $\Delta H_{m100\%}$]. The reference melting enthalpy of PET with 100 % crystallinity was 140.1 J/g [31].

2.6. Comparison of different toughening additives

The boundary for this one-pot modification process was developed through a cradle-to-gate system to acquire benzoate ethyl lignin derivatives as targeted products. The system consisted of four steps, including the drying process (step a), the chemical modification process (step b), the fractionation and washing process (step c), and the distillation process (step d). Each single process step is calculated separately to obtain the input and output numbers of materials and energy consumption for developing a life cycle inventory (LCI) (Supplementary Table 1). The local electricity mix provided the input energy. Detailed information is described in the supplementary materials. The PET types (recycled vs virgin) and processing methods (e.g., draw ratio and blending time) can affect their mechanical performance. Therefore, their toughening impacts, considering the strength, modulus, and elongation at break, were first normalized to make them comparable (Supplementary Table 2 and Table 3). We assumed all these filaments were processed by the same thermal–mechanical blending under the conditions described in this study. The changing mechanical performances will also affect the consumption of materials to meet the strength requirement of an application. Their density differences by adding specific toughening additives may impact the GHG emission when preparing the final PET composite. Combined all of these factors, we then develop an equation (1) to re-elucidate the GHG emission of PET composite (GHG_{PC}) and compare it with the PET (equation (2) to understand the impacts of different additives in percentage (GHG %) [32].

$$GHG_{PC} = [GHG_P \times (1 - W_t) + GHG_t \times W_t] \times \frac{\rho_{PC}}{\sigma_{PC}} \quad (1)$$

$$GHG\% = \frac{GHG_P \times \frac{\rho_P}{\sigma_P}}{GHG_{PC}} \times 100\% \quad (2)$$

3. Results and discussion

3.1. One-pot route to synthesize and fractionate benzoate ethyl lignin building blocks

Valorization of heterogeneous kraft lignin requires effective and green modification methods to add desired functional groups, improve their uniformity (lower molecular weight and its distribution), and increase their thermal stability. The BELignin building blocks are synthesized through a one-pot process developed in our previous studies (Fig. 1). Ethylene carbonate (EC) can selectively convert aromatic hydroxyl (Ar-OH) and carboxylic acid (COOH) groups into primary aliphatic hydroxyl (Al-OH) groups [33]. Notably, the reaction times can be changed while working with lignin from different isolation methods or species. Our previous studies have indicated that the CO_2 gas production rate (or reaction rate) has a stoichiometry correlation with the degree of modification [34]. A real-time monitoring instrument was developed to analyze the CO_2 gas production rate or reaction rate (Supplementary Figure 1). Fig. 1**a** shows the reaction kinetics, indicating the reaction consists of four stages that are affected by different factors: the solubility of lignin (stage 1 and stage 2), the amount of reactive groups (stage 3), the viscosity of reaction mixtures (stage 4), or their combination. At stage 4, the reaction rate reaches 0.1 – 0.2 ml min^{-1} (Stage 4), indicating that reactive groups (phenol and carboxylic acid) in

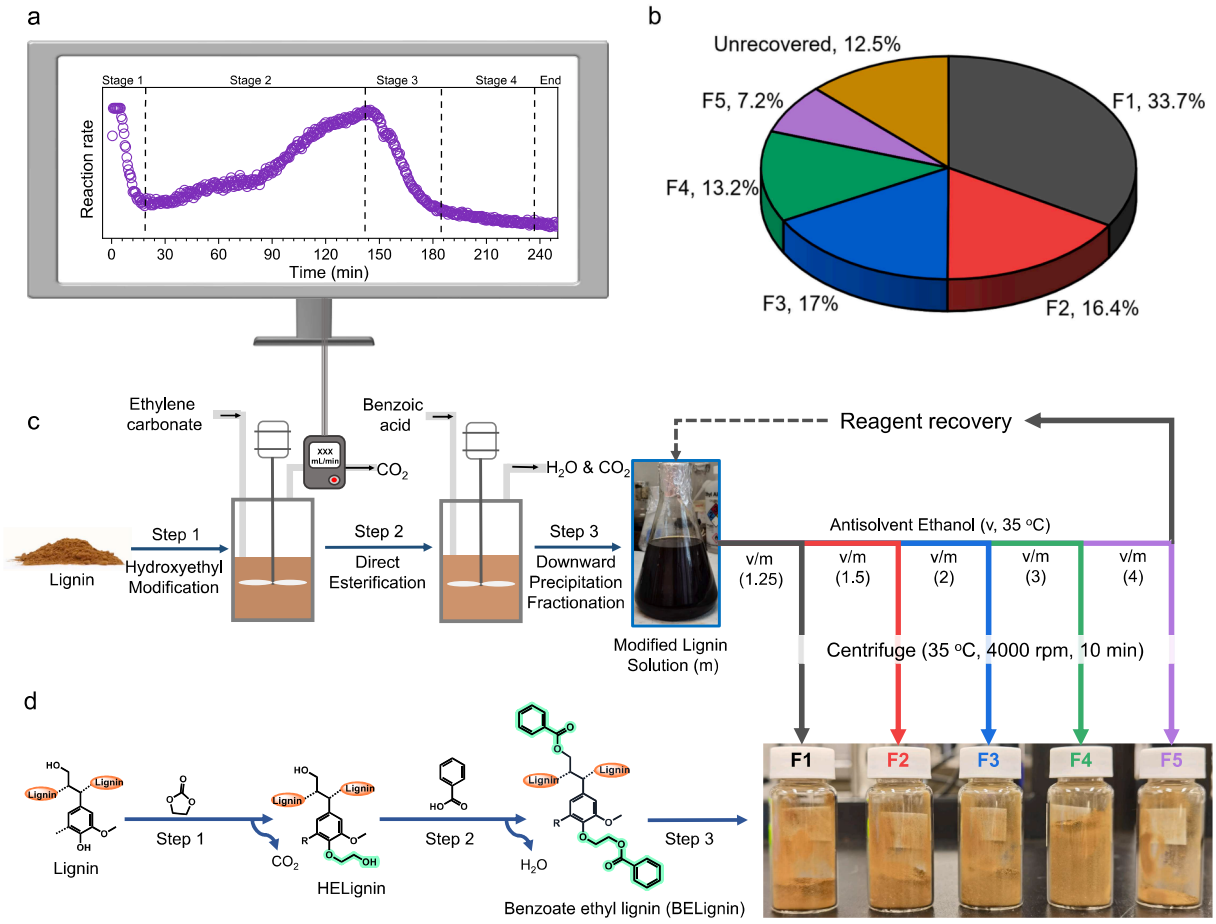

Fig. 1. A simple and digitalized chemical modification process to acquire benzoate ethyl lignin derivatives (F1-F5). (a) CO_2 gas production rate associated with the reaction time during the hydroxyethyl modification (step 1, reaction condition: 120 °C, real-time monitoring, and solvent-less conditions); (b) Mass distribution of different BELignin fractions; (c) and (d), the scheme of the one-pot process including the hydroxyethyl modification (step 1), direct esterification (step 2, reaction condition: 170 °C, 48 h, and solvent-less conditions), and the downward precipitation fractionation (step 3); v/m is the ratio between the volume of antisolvent (ethanol) and the mass of reaction mixtures; reagent recovery process aims at acquiring the ethanol and major side products from benzoate ethyl derivatives.

lignin have been consumed completely. We can then stop the reaction promptly, allowing us to improve its consistency, control the quality of modified lignin, and reduce optimization efforts.

While the hydroxyethyl reaction is finished, benzoic acid is directly added to the mixture for the subsequent esterification with the aliphatic hydroxyl (Al-OH) group (Step 2). Noteworthy, ending the hydroxyethyl reaction promptly is crucial to improving the solubility of hydroxyethyl lignin in organic acid. Step 2 is a solventless process in which an excess amount of organic acid is required to solubilize the lignin and react with the excess amount of EC and alkali catalyst, leading to an extended reaction time (48 h) [35]. The downward precipitation fractionation (Step 3) is performed to recover BELignin (F1 – F5) with specific molecular weight (Fig. 1**c and d**). Flory-Huggin's equation shows that the solubility parameter of polymers is directly related to their degree of polymerization (or molecular weight) [36]. With a good solvent (benzoic acid and ethylene carbonate), we can gradually decrease the solubility parameters by adding antisolvent (ethanol) and precipitate lignin with a specific molecular weight (F1-F5). The different fractions have weight distributions ranging from 7.2 % to 33.7 % (Correct yield, Fig. 2**b**). The correct yield is calculated considering the effects of additional benzoate ethyl groups [25].

3.2. *Cradle-to-gate life-cycle carbon analysis*

A simple cradle-to-gate life cycle assessment was performed to understand the greenhouse gas emission in producing 1 kg benzoate ethyl lignin derivatives (Fig. 2). The process consisted of four steps: the drying process (a), chemical modification (b), fractionation and washing (c), and distillation (d). Carbon emission for each step will include transporting raw materials and chemicals, energy consumption, and preparing original materials and reagents. The laboratory scale process (10 g) was scaled up to a processing quantity of 1 kg kraft lignin following the framework developed by Som and her collaborators [37]. Overall, GHG emission in making 1 kg of benzoate ethyl lignin (BELignin) derivatives is calculated to be 1.56 kg eq CO_2 kg. 51.2 % of carbon emissions are attributed to the drying (a) and distillation process (b) to recover ethanol or remove lignin moisture. The modification process can produce 19 % of carbon emissions. The energy consumption for the downward precipitation fractionation process is negligibly low indicating this it is promising to fractionate lignin during the recovery (Supplementary Table 1).

The ethanol in the final supernatant (fraction 5) was recovered by a roto evaporator and measured to calculate the mass balance of our one-pot esterification process. The solid residues were analyzed by TGA (**Supplementary Figure 2**) and NMR (**Supplementary Figure 3**).

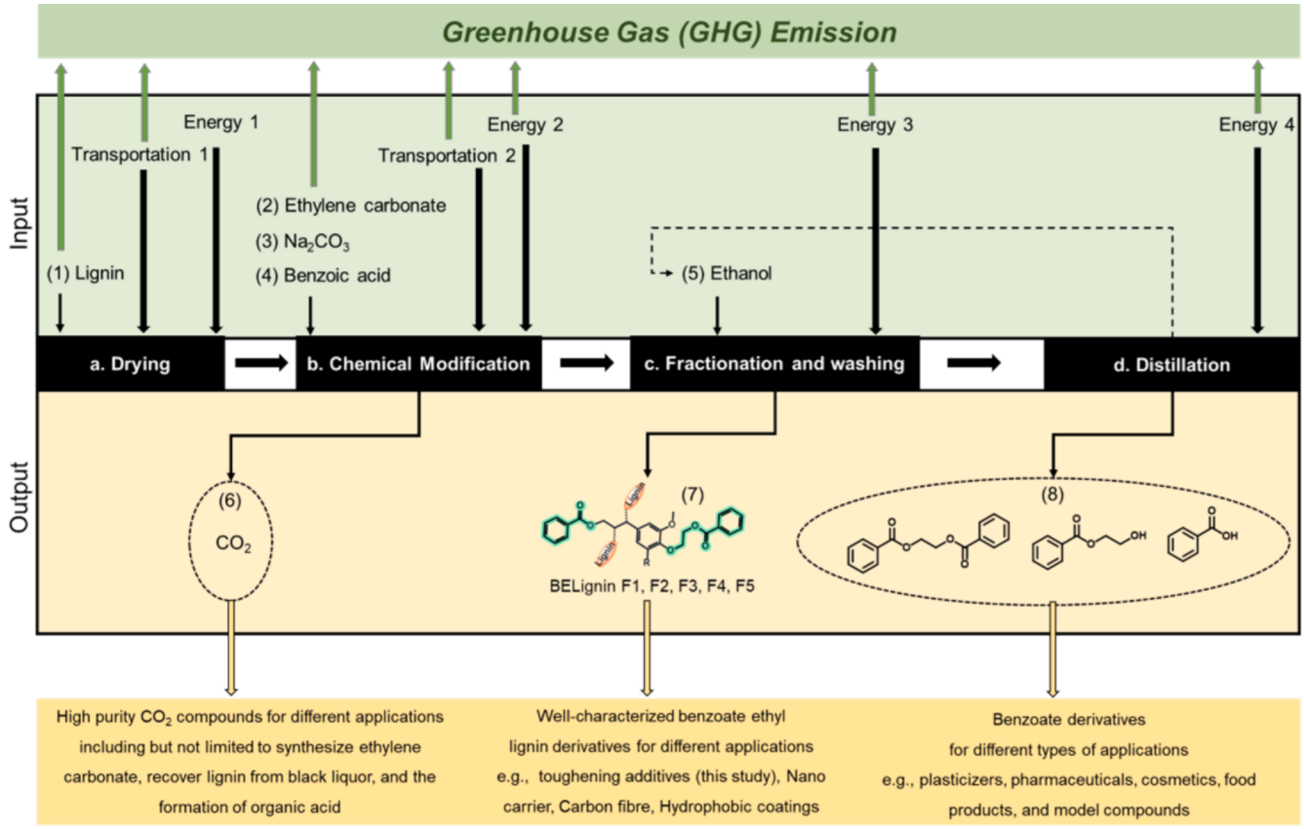

Fig. 2. Input and output of the one-pot modification process in producing targeted products (7) benzoate ethyl lignin derivatives (BELignin), co-products including high purity CO2 (6) and benzoate glycolate (8), and its Greenhouse Gas Emission.

Results show that the major components in the solid residue are benzoic acid and benzoic acid derivatives. In other words, lignin loss (12.5 %) is due to the recovery and washing process. The other valuable products during this process include high-purity CO_2 (7) and benzoate ethylene glycol derivatives (8), as verified by the ^{13}C NMR (**Supplementary Figure 3**). The CO_2 can be used as a real-time monitoring process analysis detector. It can be easily collected and reused to prepare organic or sodium carbonate [38] or recover the lignin from black liquor [34,39]. On the other hand, co-products, including benzoate derivatives, have valuable applications in chemicals and materials (e.g., plasticizers [40] and model chemicals) (Fig. 2). The utilization of these co-products can potentially lower carbon emissions significantly and further improve the environmental footprint of making benzoate ethyl lignin derivatives.

3.3. Characterization of benzoate ethyl lignin derivatives

These five benzoate ethyl lignin (BELignin F1 − F5) derivatives were thoroughly characterized by GPC combined with multiple detectors (MALS + IV + dRI). All fractionated BELignin shows narrow and normalized peaks compared to unmodified lignin (Supplementary Figure 4). Their molar mass traces show a progressive shift towards a longer retention time from F1 to F5 (Fig. 3**a**). The BELignin F1 has the largest molar mass (M_n = 44.1 kDa), which is 6.6 folds of BELignin F5 (M_n = 6.7 kDa), and 10 folds of unmodified lignin (M_n = 4.0 kDa). All BELignin (Đ =2.5——1.1) have enhanced uniformity compared with kraft lignin (Đ=7.6) (Supplementary Table 4). The Mark-Howink-Sakurada (MHS) plots (**Supplementary Figure 5**) highlight the relationship between the molar mass and the intrinsic viscosity of the lignin macromolecule. The slope of the MHS plot indicates the conformation of the polymer [28]. The higher α-value indicates a more extended conformation of lignin in the solvent [28]. All BELignin fractions have an α-value less than 0.5 (means more flexible polymers) (Fig. 3**b**), and the α-value for F3 (0.08), F4 (0.14), and F5 (0.14) are quite small, suggesting that they are more densified spheres in DMSO solvent [25]. The α-value of F1 and F2 are 0.39 and 0.45, meaning they have a more extended structure, likely ellipsoid.

To characterize the effectiveness of modification, including hydroxyethyl reaction and direct esterification, the amount of Al-OH, Ar-OH, and COOH groups for the lignin and BELignin (F1-F5) were quantitatively analyzed by ^{31}P NMR (Supplementary Figure 6). The results show that the amount of these functional groups in BELignin decreased markedly, suggesting a high efficiency of the modification; the degree of substitution (DS) was calculated based on the changing amount of hydroxyl groups, ranging from 83.9 % to 84.8 % (Fig. 3**c**). ^{13}C NMR spectra of BELignin F2 and unmodified lignin show newly formed benzoate ethyl groups on the lignin surface, further testifying the two-step modification process. (**Supplementary Figure 12a**) Nonetheless, all BELignin fractions still contain a small amount of Ar-OH (0.4 mmol/g) and Al-OH groups (0.6 mmol/g). BELignin F5 has more Ar-OH groups than other BELignin fractions (Supplementary Table 5). We understand that phenols on the lignin surface can play multiple functions, such as antioxidant properties. Keeping a certain amount of these groups can assist with the mechanical reprocessing of lignin-based composite for circular plastics.[41].

The thermal stability of lignin can have dramatic effects while blending with PET; PET's melting temperatures are typically above 260 °C, which is higher than $T_{d5\%}$ for unmodified lignin. After the modification, all BELignin displays similar thermal gravimetric curves (Fig. 3**c**). The decomposition temperature at 5 % weight loss of BELignin ($T_{d5\%}$ = 296 – 306 °C) is much higher than the unmodified lignin ($T_{d5\%}$ = 234 °C) as well as the corresponding melting temperature of PET

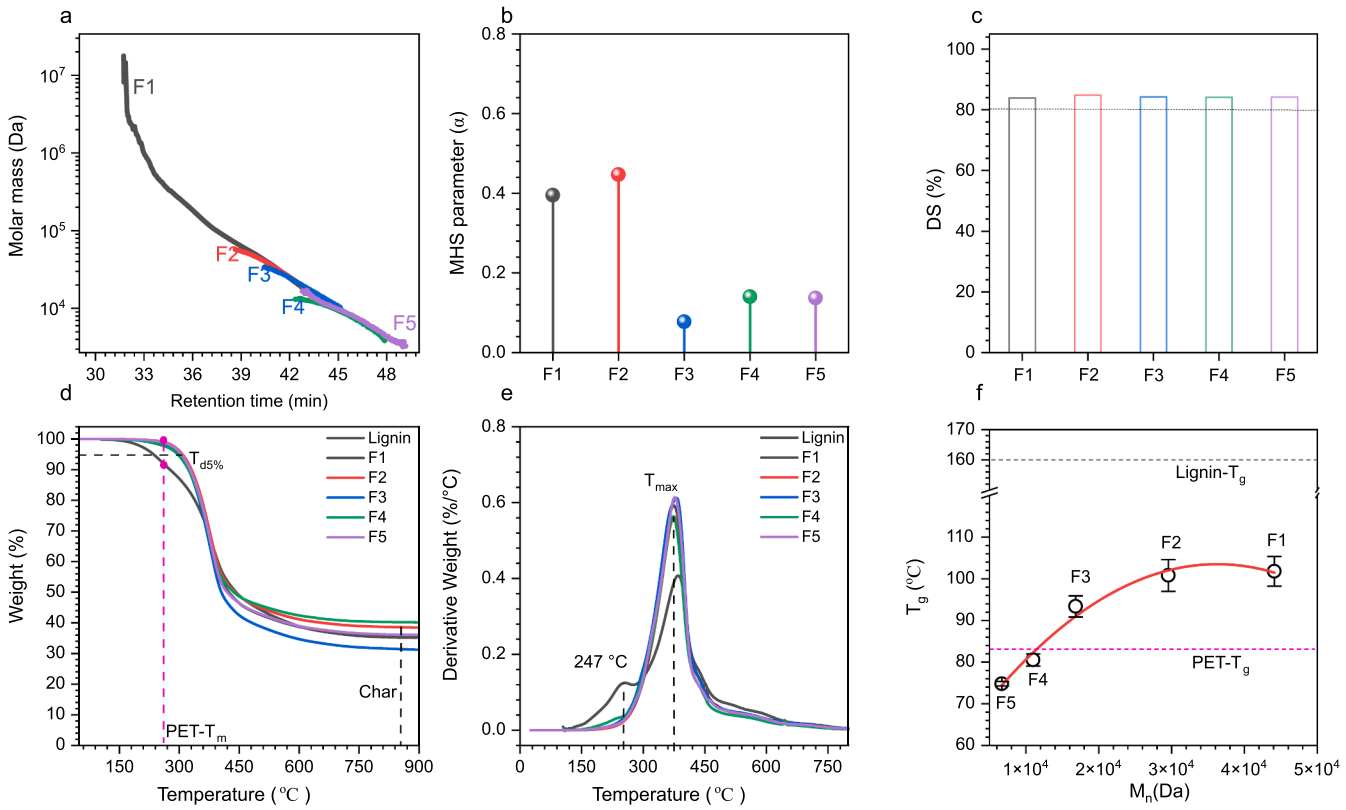

Fig. 3. Characterization of fractionated benzoate ethyl lignin derivatives. (a) molar mass traces of fractionated benzoate ethyl lignin derivatives; (b) conformation of fractionated benzoate ethyl lignin derivatives; (c) degree of substitution (DS) based on changing amount of hydroxyl groups from ^{31}P NMR spectra; (d) thermal gravimetric analysis of lignin and BELignin (F1 – F5); (e) derivatized thermal gravimetric analysis of lignin and BELignin (F1-F5); (f) glass transition temperature aligning with the number average molecular weight (M_n) for different BELignin and their comparison with PET (red dash line) and unmodified lignin (dark dash line). (For interpretation of the references to color in this figure legend, the reader is referred to the web version of this article.)

(PET-T_m = 260 °C) (Fig. 3**d**), because a decreasing amount of hydroxyl groups can minimize the related dehydration under this temperature. Also, etherified lignin units are more stable than free phenolic counterparts, which helps support thermal stability. While lignin powders were further heated between 300 °C and below 500 °C, the decomposition temperature at the maximum weight (T_{max}) (374.1 – 380.5 °C) is close to the kraft lignin (385 °C) (Fig. 3**e**). It suggests that the derivatized modification does not change the backbone structure, such as the aromatic ring and propane side chains [42]. The DSC was applied to analyze the T_g of different lignin fractions. The curves showed that F1 has a broader glass transition temperature window than the other fractions, attributed to its wider molecular weight distribution. The T_g (74.8——101.8 °C) of BELignin is lower than unmodified lignin (160 °C) but near the T_g of PET (83 °C) (Fig. 3**f**).[25] Like petroleum-based thermoplastics [43], the T_g of fractionated BELignin is highly correlated with the molar mass (M_n) (**Supplementary Figure 8**); an increasing M_n has a higher T_g until reaching 100 °C while the T_g becomes independent of M_n (Fig. 3**f**). These results further verified the efficiency of our precipitation fractionation process to acquire lignin with different molar mass.

3.4. Fabrication of LignoPET filaments

We used a twin-screw extruder combined with a fiber take-up line to fabricate a series of filaments (diameters = 200——300 μm) (Fig. 4**a** and **Supplementary Figure 9a-c**). Fibre and filaments described here can potentially have applications in the textile industry or 3D printing filaments [44]. As with the PET, adding BELignin results in continuous, strong, and smooth PET filaments more than 145 m long, indicating excellent compatibility between PET and BELignin derivatives (Fig. 4**a and Supplementary Figure 9c**). In contrast, filaments produced with unmodified lignin are brittle, have an irregular surface, and quickly fail during collection (**Supplementary Figure 9b**). It shows large lignin particles on the surface (more than 100 μm). Additionally, while compounding unmodified lignin with PET, there is an odorous sulfur-related scent due to the unwanted fragmentation of the lignin at this high temperature [45]. Conversely, no odorous scent was released for BELignin during compounding, a significant breakthrough for melt-processed kraft lignin materials. This is because the hydroxyethyl modification can partially remove the sulfur content in lignin [34].

3.5. Mechanical performances of LignoPET filaments

The stress–strain curves of each filament are acquired to evaluate the impacts of different lignin additives on their tensile properties (Fig. 4). During the straining of these filaments, the linear elastic deformations first appear until the yield point – the force then causes non-recoverable plastic deformation (Fig. 4**b**). At this stage, we can visually find plastic deformation accompanied by clear whitening (necking) just before the fracture of filaments, indicating a rupture mechanism involving crazing and crystallization. This phenomenon is more evident in the LignoPET (Lignin) due to the debonding between unmodified lignin and PET matrix and the formation of cavities. Compared to PET, blending unmodified lignin reduces the mechanical performance of PET filaments, i.e., lowered Yield strength by 14.84 % (Fig. 4**c**), Young's modulus by 11.8 % (Fig. 4**d**), and yield strain by 15.62 % (Fig. 4**e**). Conversely, BELignin additives markedly enhance the mechanical performances; Young's modulus increased by 6.34 % ~ 27.19 %, and yield stress

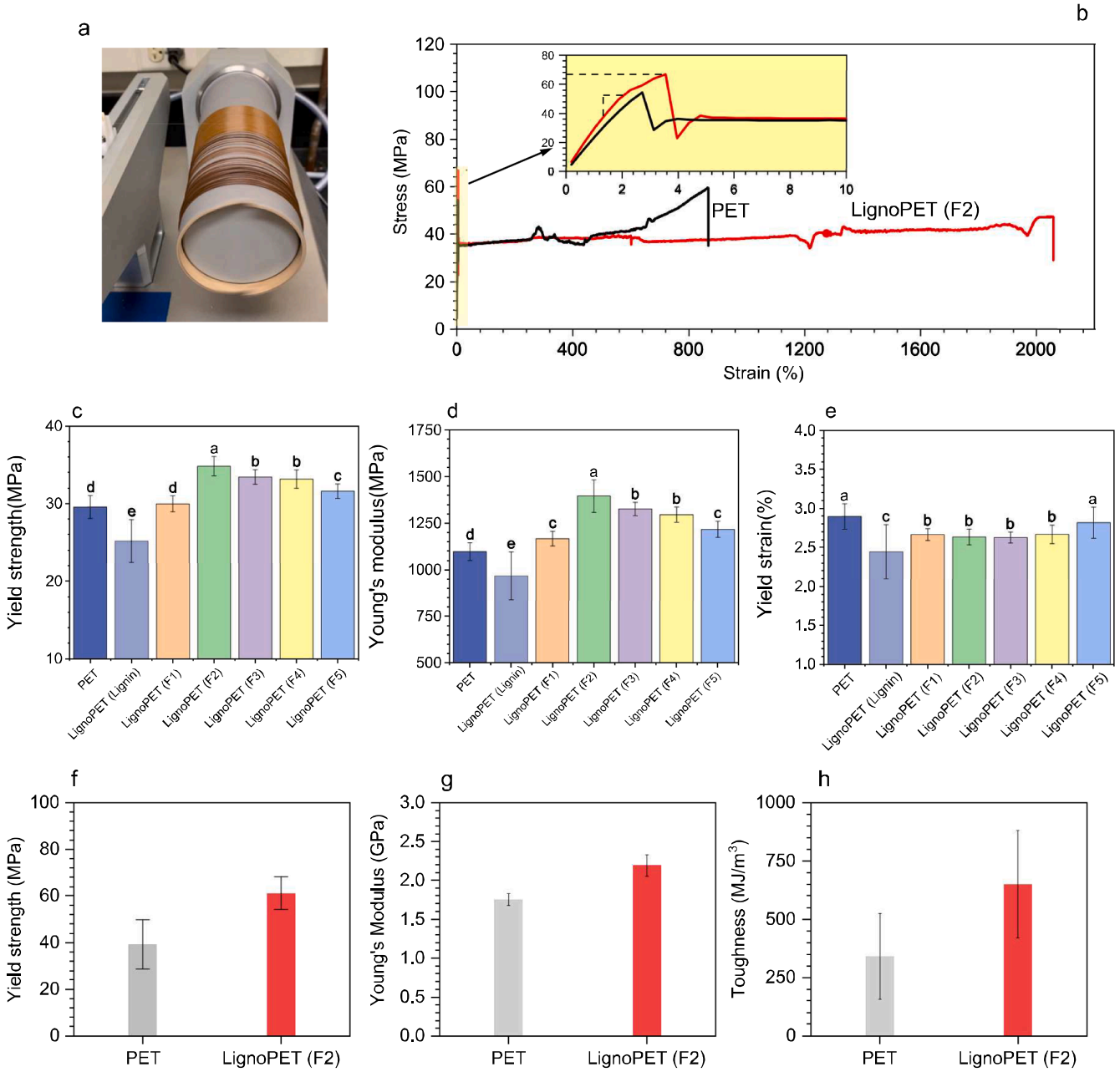

Fig. 4. Mechanical performances of PET and LignoPET filaments. (a) LignoPET (F2) filaments; (b) tensile stress and strain curves of PET and LignoPET (F2); DMA tests (3 N/m until reaching the maximum force 18 N) results including Yield strength(c), Young's modulus(d), and yield strain (e); and Instron tensile tests (25 mm/min until the breakage of filaments, following ASTM C1577 standard) including yield strength (f), Young's Modulus (g), and toughness (h).

increased by 1.42 % ~ 17.82 %. One-way ANOVA analysis is executed, indicating the significance of the mechanical reinforcement for all BELignin, especially for LignoPET(F2). (Fig. 4**c-e**).

We then used the Instron Tensile test instrument to acquire complete stress–strain curves for LignoPET (F2) and PET filament and understand the toughening effects of BELignin (Fig. 4**b**) according to ASTM C1577 [30]. Each filament was measured four times to understand variability. (**Supplementary Figure 10**) Due to the different stretch speeds and measuring gaps by Instron and DMA tests, the results can differ but have a similar trend, leading to the same conclusion. Adding BELignin (F2) to PET can increase the yield strength (+56 %, Fig. 4**f**) and Young's Modulus (+25 %, Fig. 4**g**). The Elongation at break also significantly increased from 921 % to 1811 %. As such, the toughness of PET can increase by 91 %, from 340.9 MJ/m^3 to 649.8 MJ/m^3 (Fig. 4**h**). These results suggest that BELignin building blocks can effectively toughen PET, representing a significant breakthrough in this area. There have been a few studies investigating lignin-based PET composites. Akato et al. tried to blend 30 % of thermal-treated kraft lignin with PET, showing dramatically decreasing mechanical performances in all properties. The acetylation of surface functional groups[46] or adding compatibilizers[47] may improve the dispersibility of lignin particles within the PET matrix. However, these can cause additional negative impacts on mechanical performances and solvent resistance toward organic solvent. It is worth noting that several other factors, such as lignin concentration, lignin structure, the type of PET, and processing, can all dramatically affect the toughening performance, making it possible to further enhance the mechanical performance, which will be optimized in our later studies.

3.6. Thermal properties of LignoPET composite

Differential scanning calorimetry (DSC) was applied to study the effects of lignin additives on the thermal properties of PET filaments (**Supplementary Figure 11**). Independent of the type of lignin, the data shows that LignoPET has 2 – 8 °C lower cold crystalline temperature (T_{cc}) than plain PET, but the temperature, enthalpy, and shape of the subsequent melting peaks are not affected by the additional lignin additives. The lignin additives can increase the temperature of the crystallization peak (T_c peak) by more than 10 – 20 °C, and the LignoPET's crystalline peaks are sharper and narrower. The reason is that lignin particles can induce nucleation of PET crystallites at a relatively high temperature, potentially increasing the population of the thin crystallites in the blend [48]. Therefore, the crystallinity (X) of LignoPET composites, ranging from 9 % to 16.6 %, is much higher than the crystallinity of plain PET (4.4 %) (Table 1). Compared with LignoPET (BELignin), LignoPET (lignin) exhibits lower T_c and T_{cc}, suggesting a lower function of induced nucleation. This could be due to the difference in agglomeration, aspect ratio, and size of lignin particles in the blending process [49]. The T_g of LignoPET (BELignin) is decreased by 2.5 – 4.6 °C, while LignoPET (lignin) exhibits a similar T_g value than that of plain PET (Table 1).

Table 1
Thermal properties of PET and LignoPET composite.

Materials	$\triangle H_{cc}$ ($J{\cdot}g^{-1}$)	T_{cc} (°C)	$\triangle H_m$ ($J{\cdot}g^{-1}$)	T_m (°C)	X (%)	$\triangle H_c$ ($J{\cdot}g^{-1}$)	T_c (°C)
PET	34.0	129.6	39.8	248.7	4.1	35.5	184.3
LignoPET (Lignin)	30.7	121.6	47.9	251.2	16.6	40.3	195.8
LignoPET (F1)	28.9	124.7	40.8	250.1	9.0	40.0	195.6
LignoPET (F2)	26.4	127.2	40.7	248.9	11.3	38.4	203.5
LignoPET (F3)	24.6	125.6	41.6	249.9	13.5	35.7	208.8
LignoPET (F4)	23.4	125.3	41.0	249.6	14.0	35.3	205.9
LignoPET (F5)	30.3	124.7	47.9	251.5	13.9	35.8	206.9

3.7. Morphologies of LignoPET composite

The compatibility of lignin with PET matrix was characterized by using optical microscopy to observe surface morphology and cross-section for LignoPET filaments. LignoPET (lignin) filament displays an uneven surface containing large brown particles (Fig. 5). Phase separation is very common when blending unmodified lignin with polymers like PET matrix, because the high blending temperature can degrade or repolymerize the lignin, forming larger lignin domain areas or particles. In contrast, all LignoPET filaments containing BELignin exhibit much smoother and homogenous surfaces and crosssection, suggesting excellent blending compatibility between BELignin and PET matrix (Fig. 5**b-f**). Polarized optical microscopy analysis distinguished the amorphous lignin in the PET matrix (Fig. 5**, bottom**). Due to the birefringence, PET crystals under the POM show interference, resulting in different colours dependent upon their order, whereas amorphous lignin particles show yellowish or dark color. When blending different BELignin with PET, we can hardly identify any lignin-rich domains within the PET matrix.

Scanning electron microscopy was applied to give more details about the micromorphology of PET filaments, LignoPET (lignin), and LignoPET (F2) (**Supplementary Figure 9** and **Video 1-3**). Unmodified lignin is blended with PET, forming large phase-separated particles (diameters 10——200 μm), irregularly embedding on the surface and at the cross-section of filaments (**Supplementary Figure 9b**). Its cross-section further indicates a more apparent phase separation of lignin particles. (**Video 2**) These results attribute to the lignin aggregation or cross-linking reactions at elevated temperatures [13], suggesting a weak interaction (physical bond) and low compatibility between unmodified lignin and PET. The SEM images show that both PET and LignoPET (F2) (**Supplementary Figure 9c**) display uniform surface and cross-section, especially when compared with LignoPET (Lignin). More images regarding their cross-section are provided (Video 3), showing the detailed distribution over the cross-section of PET filament. This is quite different compared with the neat PET (**Video 1**). 90 % of these cavities or particles have diameters less than 1 μm close to the optimal particle size range (around 0.4 μm) for toughening (Fig. 6**c**). A preferred particle size range (0.4 ± 0.2 μm) in the polymer matrix was revealed to realize the reinforcement for semi-crystalline PET [31].

3.8. Reinforcement mechanism of BELignin derivatives

The results discussed above showed that BELignin has enhanced thermal stability ($T_{d5\%}$>T_m-PET), as we functionalize the hydroxyl groups with benzoate ethyl groups. This group is like the fundamental units in PET, positively influencing their compatibility with the PET matrix. Its polydispersity index is reduced to improve its uniformity and show a more predictable T_g, close to the T_g of PET. Its conformation also changed depending on the molecular weight; larger molar mass lignin shows a more extended structure than low molar mass ones. These newly structural features of BELignin can markedly influence PET's crystallization behaviour by incurring crystalline formation at a high temperature, which may modify the density and size of PET crystallites. Multiple structural features, such as extended structure, surface functional groups, as well as a uniform molar mass distribution, can positively impact the particle size distribution in the PET matrix and contribute to investigating how the lignin structure or thermal properties affect the performance of the LignoPET composite.

LignoPET composite attains increasing strength (+56 %), Young's modulus (+25 %), Elongation at Break (+95 %), and toughness (+91 %), simultaneously (Fig. 4). Due to its branched and rigid structure and enriched aromatic units, technical lignin has a high Young's modulus () that can increase the Young's modulus of the resulting composite. The enhancement of strength and elongation at break are attributed to multiple crazes in the polymer matrix, which can spread over a large matrix volume [11]. The high-resolution SEM image for LignoPET (**Video 3** and Fig. 6**b**) shows the overlap of cavities. Previous stress field

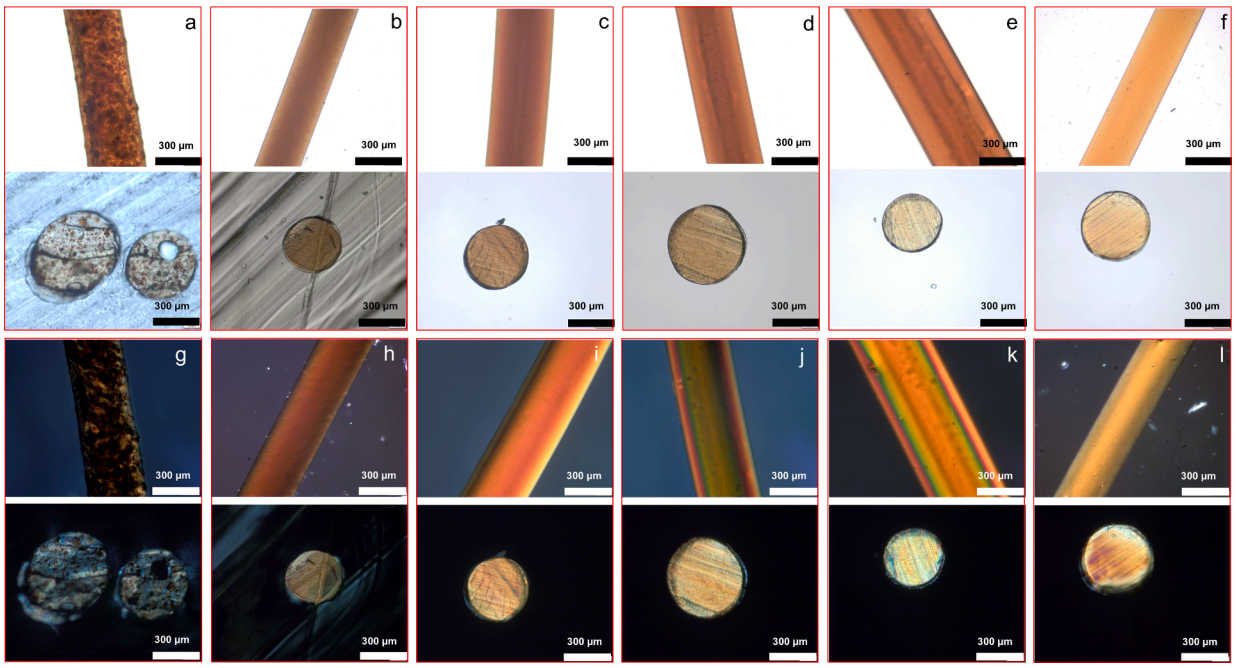

Fig. 5. Optical micro-morphology LignoPET filaments containing lignin (a), BELignin F1 (b), BELignin F2 (c), BELignin F3 (d), BELignin F4 (e), or BELignin F5 (f) and polorized optical microscopy.

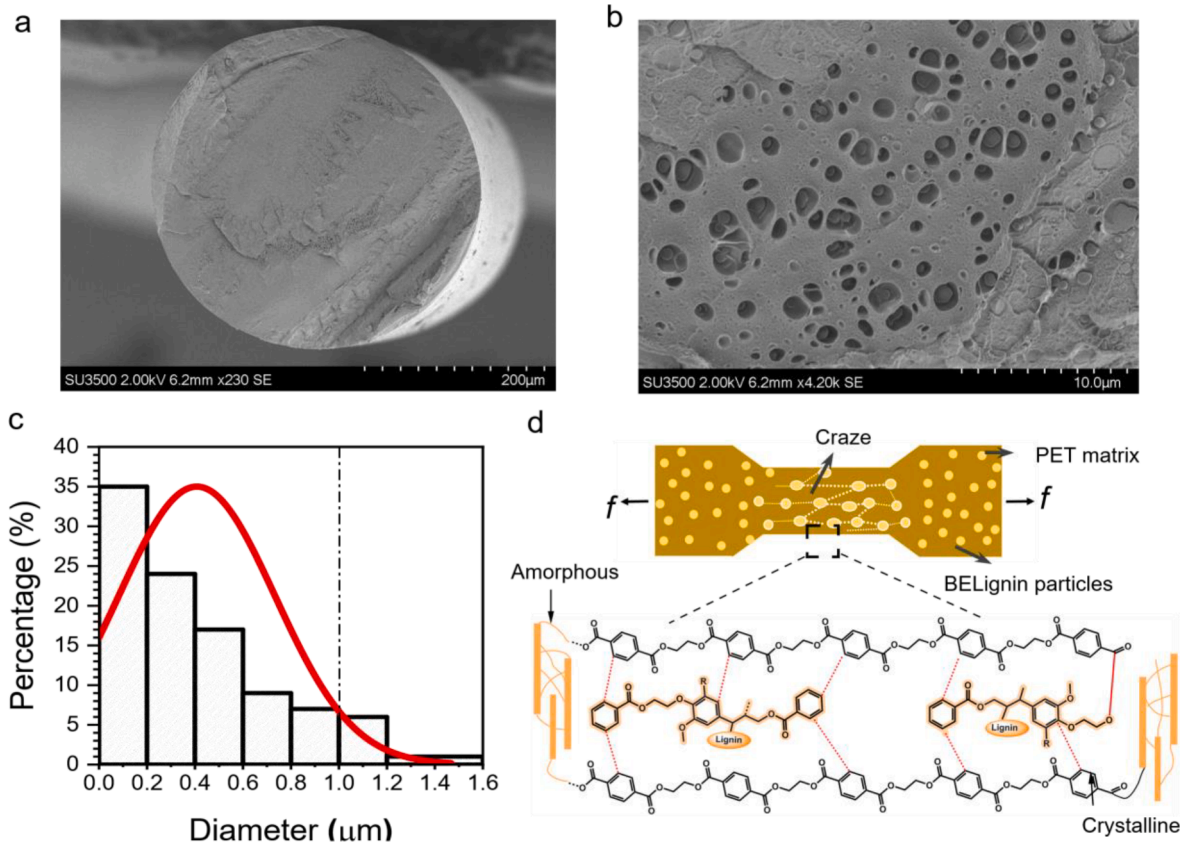

Fig. 6. Morphology of and cross-section of LignoPET composite containing BELignin F2 (a, b); **(c)** the particle size distribution of BELignin F2 in PET filaments (c); the reinforcing mechanism of BELignin-based toughening additives (d).

models and oriented layer model [50] discussed that these morphological features could cause the cracks to percolate over the entire polymer matrix, offering a path for plastic deformation propagation. In other words, there is still space to improve toughness impacts by optimizing the additive concentration and processing parameters. Large lignin microparticles for unmodified lignin are observed due to self-aggregation

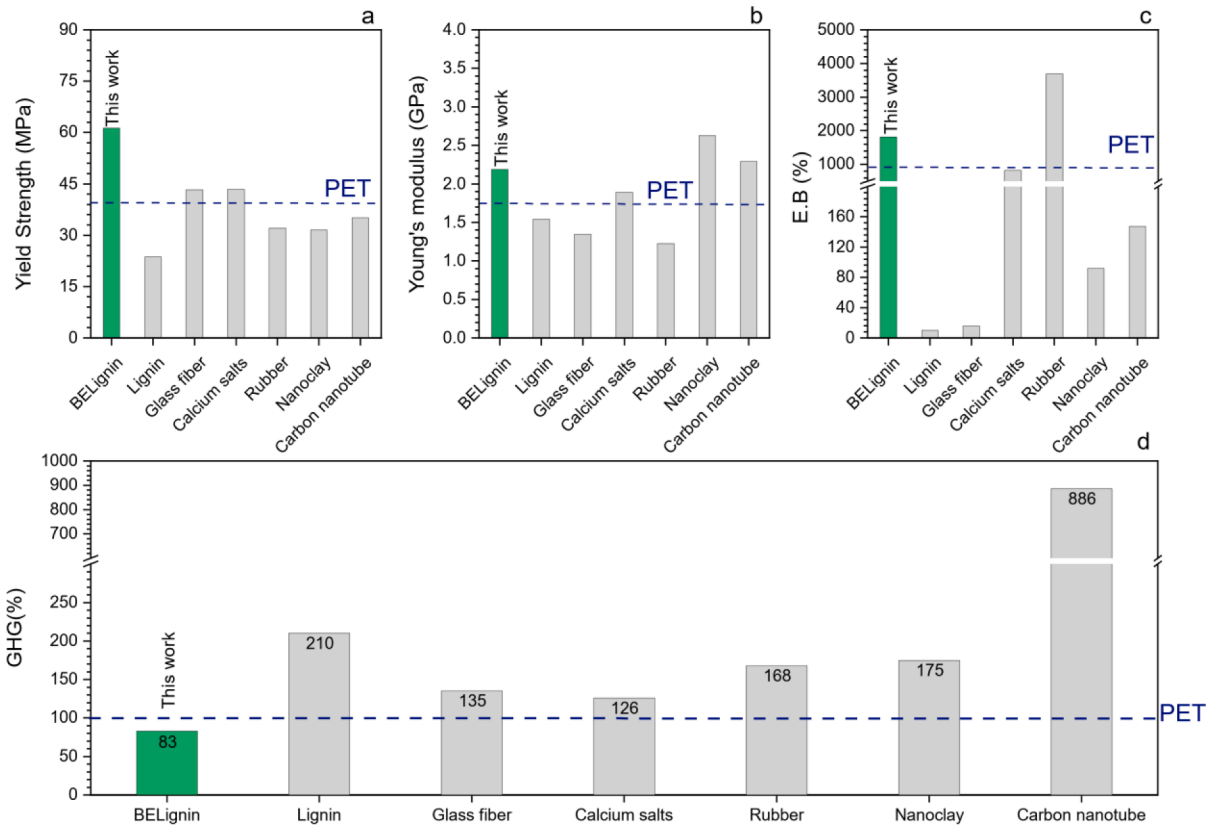

Fig. 7. Mechanical properties and environmental footprint of BElignin. Comparison BELignin (F2) (this work) with other toughening additives (lignin, glass fiber, calcium salts, rubber, nanoclay, and carbon nanotube) concerning impacts on the **(a)** strength, **(b)** Young's modulus, **(c)** elongation at break (E.B. %), and **(d)** carbon footprint (i.e. Green House Gas Emission, GHG) concerning the impacts of functional amounts, the density and amount of renewable toughening additives (as displayed in supplementary **Table 3**). (For interpretation of the references to color in this figure legend, the reader is referred to the web version of this article.)

(π-π and hydrogen bond), crosslinking reaction, and even transesterification with the PET. ^{13}C NMR spectra for the PET and LignoPET (F2) were acquired to analyze the functional groups on the lignin surface; a piece of evidence is that the benzoate groups (peak 3) have disappeared or shifted, which may be attributed to the transesterification (Supplementary Figure 12).

3.9. Comparison with typical toughening agents

For comparison, traditional toughening additives, including synthetic rubbers and nanofillers (e.g., nanoclay, carbon nanotubes, glass fibre, and calcium salts), are summarized in Fig. 7**a-c** and Supplementary Table 2. It is worth mentioning that the mechanical performances of PET can be affected by various factors such as the producers, collecting methods, and extruding conditions. So, the average toughening impacts for these additives are normalized based on the PET in this study (Supplementary Table 3). Synthetic rubbers can increase the elongation of break of PET composite by 300 % but lower their strength and modulus. Nanofillers can increase either modulus or strength or both of them. However, these fillers often decrease the elongation at break, as there is a lack of required interfacial adhesion between fillers and PET matrix (Fig. 7**a-c**) [12].

We then compare the environmental footprint of BELignin with the conventional PET additives. Compared to plain PET, LignoPET (BELignin) can lower GHGs by 17 % due to its renewable raw materials, environmentally friendly synthetic approaches, and toughening impacts (Fig. 7**d**). In contrast, all the other toughening additives will increase their GHGs from 26 % to 7-fold. For synthetic rubber, their toxic fossil-based precursors (styrene, butadiene, and acrylic acid) and functionalization approach using epoxy and anhydride chemicals will lead to more

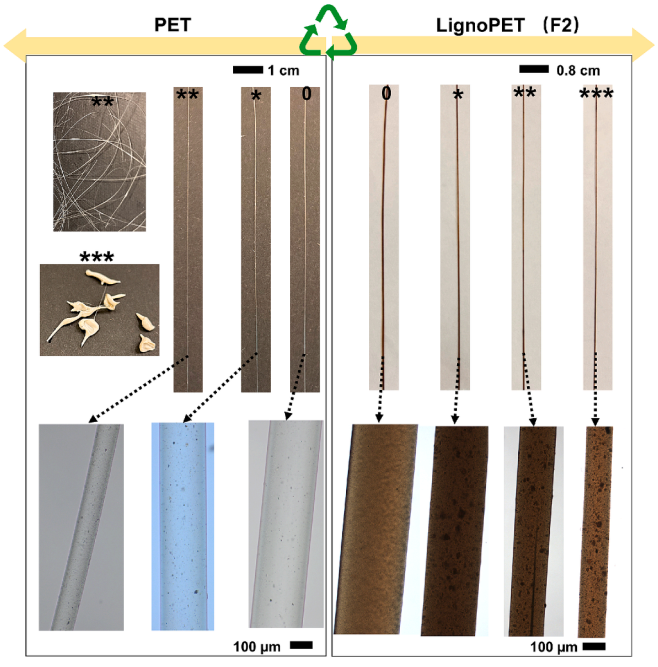

Fig. 8. Images on Macro- (up) and Micro- (bottom) morphologies of thermal recycling PET and LignoPET (F2) filaments; 0 represents original filaments, * represents recycling one time, ** represents recycling two times, *** represents recycling three times.

environmental issues [51]. Nanofillers from inorganic compounds have attracted increasing attention recently, but these fillers may lead to concern regarding decreasing environmental resistance, as they may leach out over time and contaminate the surrounding environment while increasing its brittleness [52]. As a comparison, solubility tests showed that our BELignin phases were stable in the PET matrix and did not dissolve in organic solvents that readily dissolved lignin derivatives (**Supplementary Figure 13**).

3.10. Circularity of LignoPET composite

Another benefit is the existence of phenolic groups in BELignin allows lignin to be used as an anti-oxidant reagent, precluding the formation of peroxyl radicals by reaction with oxygen [26]. It can lead to another breakthrough in improve the circularity of PET plastics as testified in this study. We investigate how BELignin affects reprocessing by the mechanical recycling process (Fig. 8). Our tests indicate that LignoPET can be easily recycled at least three times and reprocessed into filaments. Interestingly, there have particles accumulation showing on the PET surfac; this can be either from the aggregation of lignin particles or the coagulation of degraded PET chains, which require further investigation in our future studies. In contrast, the plain PET after multiple-times thermal blending, will form non-uniform filaments and droplets, attributed to the PET depolymerization [53]. This represents an important breakthrough in fabricating circular plastic materials. The 2024 PPWR regulation sets a high bar for recyclability, mandating that by 2038 only packaging materials with $\geq$ 80 % recyclability will be permitted. This study aims to upcycle PET by incorporating renewable functionalized lignin, potentially extending PET's life cycle and broadening its applications beyond lower-value products.

4. Conclusion

Branched lignin macromolecules, after modification, suggest excellent potential for modifying plastic materials (e.g., reinforcement) and positively reducing their environmental carbon footprint. Optimal structures of lignin with more extended conformation, along with chemical modification that matched PET, showed enhancement of all the mechanical properties of PET. This work created uniform BELignin building blocks, which toughened PET and enhanced its recyclability, opening an avenue to more valuable applications from this ubiquity of plastic, either reducing the specific amount needed for applications or enhancing its recyclability; in both scenarios, the carbon footprint of PET is decreased through the use of this biopolymer. These results verified our hypothesis that the structure of lignin plays a pivotal role in their subsequent applications. Other technical lignins can have low molar mass and compact structures, such as shown by multi-angle light scattering (MALS) and small-angle neutron scattering (SANS). In these cases, lignin structure features relative to their source (species) and isolation method will impact their performance in new materials [54–56]. The inherent properties of lignin polymers, including UV absorption, barrier, antibacterial, and radical scavenging, are expected to introduce advanced multi-functionalities to the PET materials such as flame retardancy, abrasion resistance, and antistatic properties, which can be critical in applications like carpeting and upholstery. These will be investigated in upcoming studies where lignin design can tailor final properties of the materials. The unique structure design will empower BELignin to be broadly used in blending with various aliphatic–aromatic polyesters [57] and positively impact their performances, which may have applications [58–60] in 3D printing filament, fibre spinning, or carbon fibre production, increase the use of the renewable resources and improve the social sustainability of plastics [61].

CRediT authorship contribution statement

Xue Wan: Writing – review & editing, Writing – original draft, Resources, Project administration, Methodology, Investigation, Formal analysis, Data curation. **Li-Yang Liu:** Writing – review & editing, Visualization, Validation, Supervision, Project administration, Methodology, Investigation, Formal analysis, Conceptualization. **Muzaffer A. Karaaslan:** Writing – review & editing, Writing – original draft, Visualization, Supervision, Resources, Methodology, Investigation, Formal analysis, Data curation. **Qi Hua:** Validation, Methodology, Investigation, Data curation. **Fei Shen:** Writing – review & editing, Funding acquisition. **Mika Sipponen:** Writing – review & editing, Visualization, Supervision, Project administration, Funding acquisition. **Scott Renneckar:** Writing – review & editing, Writing – original draft, Visualization, Supervision, Project administration, Methodology, Formal analysis, Conceptualization.

Declaration of competing interest

The authors declare that they have no known competing financial interests or personal relationships that could have appeared to influence the work reported in this paper.

Acknowledgements

This study was supported by the China Scholarship Council (Grant No. 202006910092) along with funding supports for the Advanced Renewable Materials Innovation Fund from the Edwina and Paul Heller Memorial Fund, and the Canada Research Chairs Program, Tier 2, in Advanced Renewable Materials #950-232330. Funded by the European Union (ERC, CIRCULIG, Project 101075487). However, the views and opinions expressed are those of the author(s) only and do not necessarily reflect those of the European Union or the European Research Council Executive Agency. Neither the European Union nor the granting authority can be held responsible. The authors also acknowledge funding from the Knut and Alice Wallenberg Foundation (KAW) through the Wallenberg Wood Science Center.

Appendix A. Supplementary data

Supplementary data to this article can be found online at https://doi.org/10.1016/j.cej.2024.158255.

Data availability

The data that support the findings of this study are openly available in Zenodo at https://doi.org/10.5281/zenodo.14412461.

References

[1] M. Macleod, H.P.H. Arp, M.B. Tekman, A. Jahnke, The global threat from plastic pollution, Science 65 (2021) (1979) 61–65, https://doi.org/10.1126/science.abg5433.
[2] Plastics Europe, Plastics-the Facts 2022, (2022). https://plasticseurope.org/knowledge-hub/plastics-the-facts-2022/.
[3] I. Taniguchi, S. Yoshida, K. Hiraga, K. Miyamoto, Y. Kimura, K. Oda, Biodegradation of PET: Current Status and Application Aspects, ACS Catal. 9 (2019) 4089–4105, https://doi.org/10.1021/acscatal.8b05171.
[4] R.D. Allen, Waste PET: A Renewable Resource, Joule 3 (2019) 908–919, https://doi.org/10.1016/j.joule.2019.04.002.
[5] M.J. Forrest, Recycling of Polyethylene Terephthalate, De Gruyter, Berlin, 2nd edn., 2016. https://doi.org/10.1515/9783110640304.
[6] E. and Z.W.E. ClientEarth, 100% Greenwash? Green Claims on PET Beverage Bottles in Europe, 2023. https://zerowasteeurope.eu/wp-content/uploads/2023/12/ZWE_ECOS_CE_20231031_report_Green-Claims-on-PET-Beverage-bottles.pdf (accessed November 6, 2024).

[7] L.S.T.J. Korley, T.H. Epps, B.A. Helms, A.J. Ryan, Toward polymer upcycling-adding value and tackling circularity, Science 373 (2021) (1979) 66–69, https://doi.org/10.1126/science.abg4503.

[8] L.T.J. Korley, T.H. Epps, B.A. Helms, A.J. Ryan, Toward polymer upcycling—adding value and tackling circularity, Science 373 (2021) (1979) 66–69.

[9] B. Pilkington, Recycled PET Honeycomb Composites for Lightweight Car Production, (2020). https://www.azom.com/article.aspx?ArticleID=19782.

[10] European Commission, Packaging waste:EU rules on packaging and packaging waste, including design and waste management, (2020). https://environment.ec.europa.eu/topics/waste-and-recycling/packaging-waste_en.

[11] J. Wang, X. Zhang, L. Jiang, J. Qiao, Advances in toughened polymer materials by structured rubber particles, Prog. Polym. Sci. 98 (2019) 101160, https://doi.org/10.1016/j.progpolymsci.2019.101160.

[12] N.M. Barkoula, B. Alcock, N.O. Cabrera, T. Peijs, Effect of glass fibers on rheology, thermal and mechanical properties of recycled PET, Polym. Compos. 16 (2008) 101–113, https://doi.org/10.1002/pc.

[13] W.G. Glasser, About making lignin great again—some lessons from the past, Front. Chem. 7 (2019) 1–17, https://doi.org/10.3389/fchem.2019.00565.

[14] B. Jacobs, Y. Yao, I. Van Nieuwenhove, D. Sharma, G.-J. Graulus, K. Bernaerts, A. Verberckmoes, Sustainable lignin modifications and processing methods: green chemistry as the way forward, Green Chem. 25 (2023) 2042–2086.

[15] R. Rinaldi, R. Jastrzebski, M.T. Clough, J. Ralph, M. Kennema, P.C.A. Bruijnincx, B. M. Weckhuysen, Paving the Way for Lignin Valorisation: Recent Advances in Bioengineering, Biorefining and Catalysis, Angewandte Chemie - International Edition 55 (2016) 8164–8215, https://doi.org/10.1002/anie.201510351.

[16] W. Ren, X. Pan, G. Wang, W. Cheng, Y. Liu, Dodecylated lignin-G-PLA for effective toughening of PLA, Green Chem. 18 (2016) 5008–5014, https://doi.org/10.1039/c6gc01341d.

[17] W. Liu, R. Zhou, H.L.S. Goh, S. Huang, X. Lu, From waste to functional additive: Toughening epoxy resin with lignin, ACS Appl. Mater. Interfaces 6 (2014) 5810–5817, https://doi.org/10.1021/am500642n.

[18] C. Crestini, H. Lange, M. Sette, D.S. Argyropoulos, On the structure of softwood kraft lignin, Green Chem. 19 (2017) 4104–4121, https://doi.org/10.1039/c7gc01812f.

[19] W. Zhang, N. Sathitsuksanoh, B.A. Simmons, C.E. Frazier, J.R. Barone, S. Renneckar, Revealing the thermal sensitivity of lignin during glycerol thermal processing through structural analysis, RSC Adv. 6 (2016) 30234–30246, https://doi.org/10.1039/C6RA00745G.

[20] M.A. Karaaslan, M.J. Cho, L.Y. Liu, H. Wang, S. Renneckar, Refining the Properties of Softwood Kraft Lignin with Acetone: Effect of Solvent Fractionation on the Thermomechanical Behavior of Electrospun Fibers, ACS Sustain. Chem. Eng. 9 (2021) 458–470, https://doi.org/10.1021/acssuschemeng.0c07634.

[21] J. Bouajila, P. Dole, C. Joly, A. Limare, Some laws of a lignin plasticization, J. Appl. Polym. Sci. 102 (2006) 1445–1451, https://doi.org/10.1002/app.24299.

[22] L.Y. Liu, M.A. Karaaslan, Q. Hua, M.J. Cho, S. Chen, S. Renneckar, Thermo-Responsive Shape-Memory Polyurethane Foams from Renewable Lignin Resources with Tunable Structures-Properties and Enhanced Temperature Resistance, Ind. Eng. Chem. Res. 60 (2021) 11882–11892, https://doi.org/10.1021/acs.iecr.1c01717.

[23] A.J. Ragauskas, G.T. Beckham, M.J. Biddy, R. Chandra, F. Chen, M.F. Davis, B. H. Davison, R.A. Dixon, P. Gilna, M. Keller, P. Langan, A.K. Naskar, J.N. Saddler, T. J. Tschaplinski, G.A. Tuskan, C.E. Wyman, Lignin valorization: Improving lignin processing in the biorefinery, Science 344 (2014) (1979) 709, https://doi.org/10.1126/science.1246843.

[24] D.D.S. Argyropoulos, C. Crestini, C. Dahlstrand, E. Furusjö, C. Gioia, K. Jedvert, G. Henriksson, C. Hulteberg, M. Lawoko, C. Pierrou, J.S.M. Samec, E. Subbotina, H. Wallmo, M. Wimby, Kraft Lignin: A Valuable, Sustainable Resource, Opportunities and Challenges, ChemSusChem 16 (2023) 1–34, https://doi.org/10.1002/cssc.202300492.

[25] L.Y. Liu, S. Chen, L. Ji, S.K. Jang, S. Renneckar, One-pot route to convert technical lignin into versatile lignin esters for tailored bioplastics and sustainable materials, Green Chem. 23 (2021) 4567–4579, https://doi.org/10.1039/d1gc01033f.

[26] R. Gadioli, W.R. Waldman, M.A. De Paoli, Lignin as a green primary antioxidant for polypropylene, J. Appl. Polym. Sci. 133 (2016) 1–7, https://doi.org/10.1002/app.43558.

[27] L.Y. Liu, K. Bessler, S. Chen, M. Cho, Q. Hua, S. Renneckar, Data on making uniform lignin building blocks via in-situ real-time monitoring of hydroxyethyl modification, Data Brief 33 (2020) 106512, https://doi.org/10.1016/j.dib.2020.106512.

[28] L. Ji, L.Y. Liu, M. Cho, M.A. Karaaslan, S. Renneckar, Revisiting the Molar Mass and Conformation of Derivatized Fractionated Softwood Kraft Lignin, Biomacromolecules 23 (2022) 708–719, https://doi.org/10.1021/acs.biomac.1c01101.

[29] K. Bessler, Characterization of Acetone Fractionated and Unfractionated, Chemically Modified Lignin-Ecoflextm Thermoplastic Blends (2021).

[30] ASTM International, Standard Test Method for Tensile Strength and Young's Modulus of Fibers, C1557-20 (2020). https://www.astm.org/c1557-20.html.

[31] N.E. Zander, Z.R. Boelter, Rubber toughened recycled polyethylene terephthalate for material extrusion additive manufacturing, Polym. Int. 70 (2021) 742–748, https://doi.org/10.1002/pi.6079.

[32] Q. Xia, C. Chen, Y. Yao, J. Li, S. He, Y. Zhou, T. Li, X. Pan, Y. Yao, L. Hu, A strong, biodegradable and recyclable lignocellulosic bioplastic, Nat Sustain 4 (2021) 627–635, https://doi.org/10.1038/s41893-021-00702-w.

[33] L.Y. Liu, M. Cho, N. Sathitsuksanoh, S. Chowdhury, S. Renneckar, Uniform Chemical Functionality of Technical Lignin Using Ethylene Carbonate for Hydroxyethylation and Subsequent Greener Esterification, ACS Sustain. Chem. Eng. 6 (2018) 12251–12260, https://doi.org/10.1021/acssuschemeng.8b02649.

[34] L.Y. Liu, K. Bessler, S. Chen, M. Cho, Q. Hua, S. Renneckar, In-situ real-time monitoring of hydroxyethyl modification in obtaining uniform lignin derivatives, Eur. Polym. J. 142 (2021) 110082, https://doi.org/10.1016/j.eurpolymj.2020.110082.

[35] L.Y. Liu, Q. Hua, S. Renneckar, A simple route to synthesize esterified lignin derivatives, Green Chem. 21 (2019) 3682–3692, https://doi.org/10.1039/c9gc00844f.

[36] F. Francuskiewicz, Polymer Fractionation, 1994.

[37] F. Piccinno, R. Hischier, S. Seeger, C. Som, From laboratory to industrial scale: a scale-up framework for chemical processes in life cycle assessment studies, J. Clean. Prod. 135 (2016) 1085–1097, https://doi.org/10.1016/j.jclepro.2016.06.164.

[38] G.A. Bhat, D.J. Darensbourg, Progress in the catalytic reactions of CO2 and epoxides to selectively provide cyclic or polymeric carbonates, Green Chem. 24 (2022) 5007–5034.

[39] P.E.R. Tomani, The lignoboost process, Cellul. Chem. Technol. 44 (2010) 53–58.

[40] A.D. Godwin, 24 Plasticizers, in: Applied Plastics Engineering Handbook (Second Edition), 2017: pp. 533–553. https://doi.org/10.1016/B978-0-323-39040-8/00025-0.

[41] C. Pouteau, P. Dole, B. Cathala, L. Averous, N. Boquillon, Antioxidant properties of lignin in polypropylene, Polym. Degrad. Stab. 81 (2003) 9–18, https://doi.org/10.1016/S0141-3910(03)00057-0.

[42] S. Sahoo, Characterization of industrial lignins for their utilization in future value added applications, Biomass Bioenergy 5 (2011) 4230–4237, https://doi.org/10.1016/j.biombioe.2011.07.009.

[43] P.C. Hiemenz, T.P. Lodge, Glass Transition Temperature Polymer Chemistry, in: Polym Chem, 2020: p. 48. https://doi.org/https://doi.org/10.1201/9781420018271.

[44] K. Mikula, D. Skrzypczak, G. Izydorczyk, J. Warchoł, K. Moustakas, K. Chojnacka, A. Witek-Krowiak, 3D printing filament as a second life of waste plastics—a review, Environ. Sci. Pollut. Res. 28 (2021) 12321–12333, https://doi.org/10.1007/s11356-020-10657-8.

[45] S. Sen, S. Patil, D.S. Argyropoulos, Thermal properties of lignin in copolymers, blends, and composites: a review, Green Chem. 17 (2015) 4862–4887, https://doi.org/10.1039/c5gc01066g.

[46] H. Jeong, J. Park, S. Kim, J. Lee, J.W. Cho, Use of acetylated softwood kraft lignin as filler in synthetic polymers, Fibers Polym. 13 (2012) 1310–1318, https://doi.org/10.1007/s12221-012-1310-6.

[47] K.M. Akato, N.A. Nguyen, K. Rajan, D.P. Harper, A.K. Naskar, A tough and sustainable fiber-forming material from lignin and waste poly(ethylene terephthalate), RSC Adv. 9 (2019) 31202–31211, https://doi.org/10.1039/c9ra07052d.

[48] W. Loyens, G. Groeninckx, Rubber toughened semicrystalline PET: Influence of the matrix properties and test temperature, Polymer (guildf) 44 (2002) 123–136, https://doi.org/10.1016/S0032-3861(02)00743-7.

[49] P. Properties, Effect of Nucleating Agents on Physical-Mechanical Properties, Handbook of Nucleating Agents (2016) 205–215, https://doi.org/10.1016/b978-1-895198-93-5.50014-9.

[50] B.P. Panda, S. Mohanty, S.K. Nayak, Mechanism of Toughening in Rubber Toughened Polyolefin—A Review, Polym. Plast. Technol. Eng. 54 (2015) 462–473, https://doi.org/10.1080/03602559.2014.958777.

[51] V. Tanrattanakul, A. Hiltner, E. Baer, W.G. Perkins, F.L. Massey, A. Moet, Toughening PET by blending with a functionalized SEBS block copolymer, Polymer (guildf) 38 (1997) 2191–2200, https://doi.org/10.1016/S0032-3861(96)00774-4.

[52] F. Dominici, F. Sarasini, F. Luzi, L. Torre, D. Puglia, Thermomechanical and morphological properties of poly(ethylene terephthalate)/anhydrous calcium terephthalate nanocomposites, Polymers (basel) 12 (2020) 276, https://doi.org/10.3390/polym12020276.

[53] M. Del Mar Castro, A.I.A. López, M.J.A. Pernas, A.L. López, J.M.L. Latorre, M.V. G. Vilariño, Rodríguez, Assessing changes on poly(ethylene terephthalate) properties after recycling: Mechanical recycling in laboratory versus postconsumer recycled material, Mater. Chem. Phys. 147 (2014) 884–894, https://doi.org/10.1016/j.matchemphys.2014.06.034.

[54] I. Ribca, B. Sochor, M. Betker, S.V. Roth, M. Lawoko, O. Sevastyanova, M.A. R. Meier, M. Johansson, Impact of lignin source on the performance of thermoset resins, Eur. Polym. J. 194 (2023) 112141.

[55] W. Zhao, L.P. Xiao, G. Song, R.C. Sun, L. He, S. Singh, B.A. Simmons, G. Cheng, From lignin subunits to aggregates: Insights into lignin solubilization, Green Chem. 19 (2017) 3272–3281, https://doi.org/10.1039/c7gc00944e.

[56] C. Gioia, G. Lo Re, M. Lawoko, L. Berglund, Tunable thermosetting epoxies based on fractionated and well-characterized lignins, J. Am. Chem. Soc. 140 (2018) 4054–4061, https://doi.org/10.1021/jacs.7b13620.

[57] A. Avella, M. Ruda, C. Gioia, V. Sessini, T. Roulin, C. Carrick, J. Verendel, G. Lo Re, Lignin valorization in thermoplastic biomaterials: from reactive melt processing to

recyclable and biodegradable packaging, Chem. Eng. J. 463 (2023) 142245, https://doi.org/10.1016/j.cej.2023.142245.
[58] A.F. Sousa, R. Patrício, Z. Terzopoulou, D.N. Bikiaris, T. Stern, J. Wenger, K. Loos, N. Lotti, V. Siracusa, A. Szymczyk, S. Paszkiewicz, K.S. Triantafyllidis, A. Zamboulis, M.S. Nikolic, P. Spasojevic, S. Thiyagarajan, D.S. Van Es, N. Guigo, Recommendations for replacing PET on packaging, fiber, and film materials with biobased counterparts, Green Chem. 23 (2021) 8795–8820, https://doi.org/10.1039/d1gc02082j.
[59] J.A. Sirviö, M.Y. Ismail, K. Zhang, M.V. Tejesvi, A. Ämmälä, Transparent lignin-containing wood nanofiber films with UV-blocking, oxygen barrier, and anti-microbial properties, J. Mater. Chem. A Mater. 8 (2020) 7935–7946, https://doi.org/10.1039/c9ta13182e.
[60] A. Moreno, M. Morsali, J. Liu, M.H. Sipponen, Access to tough and transparent nanocomposites via Pickering emulsion polymerization using biocatalytic hybrid lignin nanoparticles as functional surfactants, Green Chem. 23 (2021) 3001–3014, https://doi.org/10.1039/d1gc00103e.
[61] M. Österberg, K.A. Henn, M. Farooq, J.J. Valle-Delgado, Biobased Nanomaterials—The Role of Interfacial Interactions for Advanced Materials, Chem. Rev. 123 (2023) 2200–2241.